

View Article Online
View Journal

ChemComm

Chemical Communications

Accepted Manuscript

This article can be cited before page numbers have been issued, to do this please use: S. Poppe, C. Chen, M. Wagner, F. Liu, Y. Cao and C. Tschierske, *Chem. Commun.*, 2025, DOI: 10.1039/D5CC04931H.



This is an Accepted Manuscript, which has been through the Royal Society of Chemistry peer review process and has been accepted for publication.

Accepted Manuscripts are published online shortly after acceptance, before technical editing, formatting and proof reading. Using this free service, authors can make their results available to the community, in citable form, before we publish the edited article. We will replace this Accepted Manuscript with the edited and formatted Advance Article as soon as it is available.

You can find more information about Accepted Manuscripts in the <u>Information for Authors</u>.

Please note that technical editing may introduce minor changes to the text and/or graphics, which may alter content. The journal's standard <u>Terms & Conditions</u> and the <u>Ethical guidelines</u> still apply. In no event shall the Royal Society of Chemistry be held responsible for any errors or omissions in this Accepted Manuscript or any consequences arising from the use of any information it contains.



Dpen Access Article. Published on 21 Ngberere 2025. Downloaded on 29/10/2025 20:52:46.

View Article Online DOI: 10.1039/D5CC04931H

COMMUNICATION

A series of three liquid crystalline cubic phases with an alternating sequence of single- and double-network structures

Silvio Poppe,^a Changlong Chen,^b Matthias Wagner,^a Yu Cao,*b,c Feng Liu,^{b,c} Carsten Tschierske*a

Received 00th January 20xx, Accepted 00th January 20xx

DOI: 10.1039/x0xx00000x

Bolapolyphiles, built of a π -conjugated bistolane core with polar glycerol groups at each end and two linear alkyl side-chains in lateral positions form a series of three different cubic network phases upon side-chain elongation, the single network "Plumber's Nightmare" ($Pm\overline{3}m$, SP), the double gyroid ($Ia\overline{3}d$, DG) and the single diamond network phase ($Fd\overline{3}m$, SD) with the DG as intermediate phase at the SP to SD transition.

Networks describe patterns of connection in many natural and artificial systems and are of significant interest as the basis of communication and data processing systems. ¹ Self-assembled supramolecular networks can transmit matter or information though space, as for example, charge carriers^{2,3} or chirality information.4 If the nodes and edges of such networks are arranged in periodic structures they can be applied as photonic crystals^{5,6} and the resulting spaces in the network meshes can find use for catalysis, storage and separation purposes.7 Liquid crystalline (LC) networks, commonly known as bicontinuous cubic phases, are structures occurring in small ranges at the transition between lamellar and columnar self-assembly of amphiphiles, as found in lyotropic (mostly aqueous) surfactant and lipid systems, 8,9 in block-copolymer morphologies 10 and in some LC phases of polyaromatic compounds with long or multiple flexible chains. 11 Most often the double gyroid network (DG) with space group $Ia\overline{3}d$ and trigonal junctions is found in these systems, but also double diamond (DD, $Pn\overline{3}m$) with tetrahedral and the double "Plumbers nightmare" (DP, $Im\overline{3}m$) cubic phase with octahedral six-way junctions are known (Fig. 1a-c).9,12 Usually they appear in small temperature and composition ranges, which makes their production and investigation challenging. Nevertheless, in some cases DD-DG transitions and in very few rare cases even the complete sequence DP-DD-DG was observed in lyotropic systems¹³ and in block copolymers. 14 In contrast to the double networks, the selfassembled single networks are extremely rare5,6 and only two of them, the SD $(Fd\overline{3}m)^{15}$ and the SP (single net "Plumbers Nightmare", $Pm\overline{3}m$), 16 have recently been found (Fig. 1e-f) as thermodynamically driven LC phase structures of precisely designed rod-like bolapolyphiles (BPs) with laterally attached alkyl chains.17 The SP phase was found for a 4-(phenylethynyl)tolane ("bistolane" = BT) rod-like compound 1/20 with glycerol end-groups and two linear n-eicosanyloxy (n = 20) chains fixed at the same side of the middle benzene ring (catechol diether, see formula in Table 1).16 To understand the effect of side-chain length on SP phase formation, compounds 1/n with shorter and longer chains (n = 18, 22 and 30) were synthesized and investigated. Surprisingly, even for this limited series, three LC networks with different cubic space groups were observed, representing the first case of a sequence SP-DG-SD, combining double and single network phases, reported here.

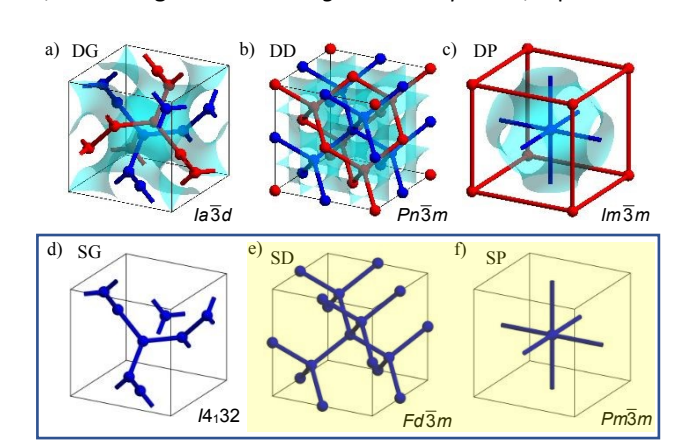


Figure 1. (a-c) Double network cubic phases with corresponding space groups and their infinite minimal surfaces (blue) and (d-f) the corresponding single networks. Reproduced from ref. 16.

The synthesis (Scheme S1, ESI) and analytical data of the new compounds 1/n with n = 18, 22, 30, and the used investigation methods are described in the ESI. The observed phase transitions and structural data of the mesophases of all compounds, including $1/20^{16}$ are collated in Table 1.

^a Institute of Chemistry, Martin Luther University Halle-Wittenberg, Kurt-Mothes Str. 2, 06120 Halle, Germany, E-mail: Carsten.tschierske@chemie.uni-halle.de

b. Shannxi International Research Center for Soft Matter, State Key Laboratory for Mechanical Behavior of Materials, Xi'an Jiaotong University, Xi'an 710049, P. R. China, E-mail: yu.cao@xitu.edu.cn

^c Institute of New Concept Sensors and Molecular Materials, Shaanxi Key Laboratory of New Concept Sensors and Molecular Materials, Xi'an Jiaotong University, Xi'an 710049, P. R. China

[†] Electronic Supplementary Information (ESI) available: [Synthesis, methods, analytical data, additional data and discussions]. See DOI: 10.1039/x0xx00000x

COMMUNICATION

This article is licensed under a Creative Commons Attribution 3.0 Unported Licence

pen Access Article. Published on 21 Ngberere 2025. Downloaded on 29/10/2025 20:52:46.

Table 1. Data of compounds **1/n**.^a

HO OH OH OH OH OH

View Article Online DOI: 10.1039/D5CC04931H

Journal Name

Compd.	Phase transitions (T/°C [ΔH/kJ·mol ⁻¹]) ^a	a/nm (T/°C)	n_{cell}	<i>n</i> _{bundle}	n _{junct}
1/18	H: Cr 93 [48.8] M 97 [5.9] Cub/ $Pm\overline{3}m$ 126 [0.8] Iso C: Iso 122 [-0.8] Cub/ $Pm\overline{3}m$ 85 [-4.7] M 76 [-63.5] Cr	3.62 (110)	28.2	9.4	56
1/20 ¹⁶	H: Cr 98 [74.8] Cub/ $Pm\overline{3}m$ 134 [1.0] Iso C: Iso 130 [-1.4] Cub/ $Pm\overline{3}m$ 79 [-78.0] Cr	3.61 (100)	26.3	8.7	52
1/22	H: Cr 101 [84.8] Cub/ $la\overline{3}d$ 148 [1.5] Iso C: Iso 141 [-0.8] Cub/ $la\overline{3}d$ 78 [-92.5] Cr	9.09 (120)	395.2	16.4	49
1/30	H: Cr 106 [100.6] Cub/ $Fd\overline{3}m$ 147 [1.4] Iso C: Iso 139 [-1.2] Cub/ $Fd\overline{3}m$ 76 [-116.6] Cr	6.74 (130)	130.6	8.2	33

^o Determined by DSC (second heating/cooling curves, 10 K min⁻¹, peak temperatures); abbreviations: $Cr = crystalline solid, Cub/Pm\overline{3}m = primitive cubic phase ("single Plumber's Nightmare", SP), Cub/<math>Ia\overline{3}d = double gyroid cubic phase (DG), Cub/<math>Fd\overline{3}m = single diamond cubic phase (SD), M = unknown LC phase, see texture in Fig. S2b (ESI); Iso = isotropic liquid, H: = data on heating, C: = data on cooling; a = cubic lattice parameter, <math>n_{cell} = molecules$ per unit cell; $n_{bundle} = number$ of molecules in the cross section of the coaxial rod bundles; $n_{junct} = number$ of glycerols in the polar spheroids; for calculation, see Table S4 and for DSCs see Fig. S1 (ESI).

Upon cooling from the isotropic liquid state, for all compounds a small exotherm in the DSC traces ($\Delta H = -0.8$ to -1.5 kJ mol⁻¹, see Tab. 1 and Fig. S1, ESI) is an indication of a phase transition within the optically isotropic phase range, which is associated with a significant increase of viscosity after crossing this transition, leading to a viscoelastic isotropic solid (Fig. S2a, ESI). Upon heating, this transition is slightly shifted to higher temperature, associated with a transition from the plastic to the fluid isotropic phase with a hysteresis of 4-8 K upon cooling (Fig. S1, ESI). In the plastic isotropic mesophase range only one diffuse scattering with a maximum at d = 0.45 - 0.46 nm is found in the wide-angle X-ray scattering (WAXS) profile for all compounds 1/n (see Figs. S3a, S5a, S7a, ESI), indicating a broad distribution of the mean distance between the molecules and molecular segments and the absence of any fixed positions of individual molecules. 11b In the small-angle (SAXS) range a series of sharp reflections confirm a periodic lattice (Fig. 2a, d, g). Both together support the LC state of this isotropic mesophase, being typical for cubic mesophases.

Three different SAXS patterns were observed for the cubic phases, depending on the chain length (Fig. 2). For compound 1/18 the SAXS patterns can be indexed to a $Pm\overline{3}m$ space group (ratio *d*-values: 1: $\sqrt{2}$: $\sqrt{3}$: $\sqrt{4}$, Fig. 3a) with a lattice parameter of a = 3.6 nm, being almost the same as reported for 1/20. The reconstructed electron density (ED) map of 1/18 (Fig. 2b) shows an electron rich (purple) cubic framework with truncated octahedral (TO) six-way junctions (ν = 6). The framework is formed by the BT units at the edges and the glycerol groups form TO 6-way junctions. The interior of this cubic framework has low ED (not shown for clarity), confirming that this space is completely filled by the low ED alkyl side-chains, excluding the possibility of an interpenetration by a second network. This confirms a network formed by fused cube-frames, leading to a simple cubic lattice with octahedral 90° junctions representing a single net of the "Plumber's Nightmare" (SP, Fig. 2c). Each unit cell is formed by 26.3 molecules, meaning that each edge of the cubic network is formed by coaxial bundles with about nine molecules in diameter ($n_{\text{bundle}} = 9.4$). At each junction six edges meet, thus 6 x $n_{\text{bundle}} = n_{\text{junct}} = 56$ glycerols form each of the polar polyhedra at the junctions (Table 1), which for simplicity are considered as slightly deformed spheres. This relatively large number of glycerols leads to a significant diameter of these polar spheres which contributes to an expansion of the lattice $(a_{\text{cub}} = d_{\text{nodes}} = 3.6 \text{ nm})$, leading to a side length of the cubes being ca. 15 % longer than the measured molecular length of L_{mol} = 2.8-3.1 nm between the ends of the glycerol groups at the BT rods (Fig. S9, ESI). This is in line with the proposed SP structure where only one bundle of coaxial BT-rods lengthwise forms the edges between the glycerol spheres. There is no significant change of the lattice parameter from 1/18 to 1/20, as it is mainly determined by the molecular (BT-rod) length. Therefore, the slightly smaller number of molecules required to fill the space in the SP lattice of 1/20 leads to a reduction of the number of parallel arranged molecules in the cross-section of the edges from 9.4 for 1/18 to 8.7 for 1/20.16

For the next homologue 1/22 the SAXS pattern changes and another cubic phase which can be assigned to an $Ia\overline{3}d$ space group (ratio of *d*-values $\sqrt{6}$: $\sqrt{8}$: $\sqrt{14}$: $\sqrt{16}$: $\sqrt{20}$...etc.) with a =9.1 nm in this case (Fig. 2d). As obvious from the reconstructed ED map (Fig. 2e) two interwoven networks with trigonal threeway junctions have high ED, as typical for double gyroid (DG) cubic network phases. In comparison to the SP structure the valence of the junctions decreases from v = 6 to v = 3 (Fig. 2f). The DG phase is formed by coaxial bundles which in this case consist of $n_{\rm bundle}$ ~16 molecules in the cross section of each network segment, in contrast to only 9 molecules found for SP. Thus, the polar junctions involve 48 glycerols which is slightly smaller than this number of $n_{\text{junct}} = 56$ (1/18) or 52 (1/20) of the SP phase (Table 1). The larger number of molecules in the cross section of the edges largely compensates the reduction of the number of attractive hydrogen bonding at the junction by the bisection of the node-valency from 6 to 3. The distance between two adjacent nodes is $d_{\text{nodes}} = a_{\text{cub}}/(2\sqrt{2}) = 3.2 \text{ nm}$ which is close to the measured molecular length L_{mol} , meaning that again a single rod-bundle is located lengthwise between the junctions (for exclusion of alternative structures, see Section S2.3, ESI).

This article is licensed under a Creative Commons Attribution 3.0 Unported Licence.

Open Access Article. Published on 21 Ngberere 2025. Downloaded on 29/10/2025 20:52:46.

Journal Name

COMMUNICATION

However, the cross section of the bundles formed by 16 molecules must become elliptical in the DG phase (see Fig. 2e) to allow all molecules to submit their chains into the aliphatic continuum. As soon as this deformation crosses a certain limiting value the DG becomes instable and is replaced by another network type.

Further alkyl chains elongation (compound 1/30) leads to a $Fd\overline{3}m$ lattice (ratio *d*-values $\sqrt{3}$: $\sqrt{8}$: $\sqrt{11}$: $\sqrt{12}$: $\sqrt{16}$:...etc., see Fig. 2g) with a_{cub} = 6.7 nm. The ED map in Fig. 2h shows a single high ED network with tetrahedral 4-way-junctions, as typical for the diamond network. The absence of interpenetration leads to the single diamond (SD) structure. Each network segment, which is still formed by only one co-axial molecular bundle in length $(d_{\text{nodes}} = (\sqrt{3}/4) \cdot a_{\text{cub}} = 2.92 \text{ nm}^{18})$ is formed by 8 molecules in the cross-section and in this case only about 32 glycerols are organized in the tetrahedral junctions. Thus, the number of glycerols forming the individual nodes decreases from 56-52 in SP via 48 in DG to 32 in SD (Table 1).

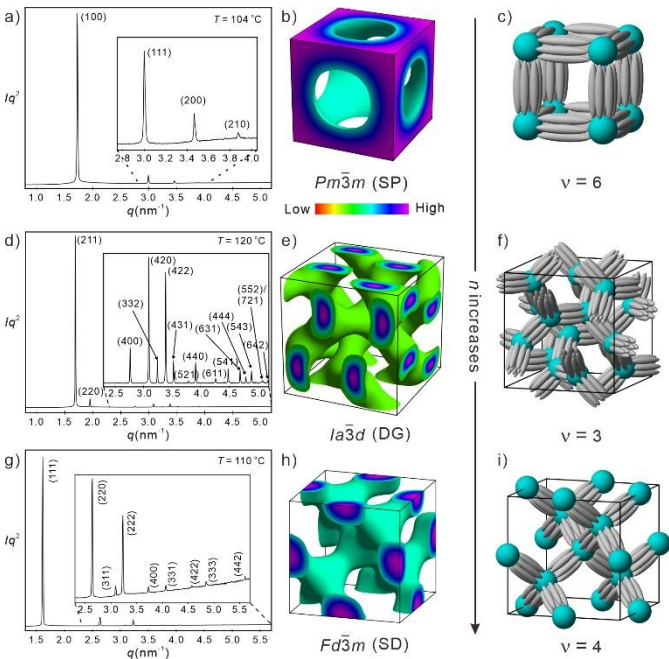


Figure 2. Cubic phases of 1/n, showing a SP-DG-SD transition by side-chain elongation. a-c) SAXS pattern of the SP phase of 1/18 with indexation and the corresponding ED map $(0\pi0\pi)$ and model showing the SP network structure, d-f) related data for the DG phase of 1/22, and g-i) the SD phase of 1/30; for details and WAXS patterns, see Figs. S3-S8 and Tables S1-S5 (ESI).

Overall the unique phase sequence of three thermotropic cubic network phases Cub/ $Pm\overline{3}m \rightarrow Cub/Ia\overline{3}d \rightarrow Cub/Fd\overline{3}m$ is found for compounds 1/n with growing chain length from n =18 to 30. Within the cubic phase sequence, the junction valence is first reduced to one half from 6 to 3 with growing side-chain volume. To allow a sufficient number of hydrogen bondings (glycerols) at the junctions to be stable they assume an elliptical shape and change the bundle cross-section from circular to elliptical (Fig. 2e). The reduced node valence is also associated with an expansion of the space available between the nets which leads to a transition from a single to a double network to retain optimized space filling. At the transition of the valence

from 3 to 4 with higher network density the interpenetration is removed again. This experimental ହଦା: found / ୦ ହେବା କରିଥି SP→DG→SD with an alternation of single and double network formation and a local minimum for the junction valence upon side chain expansion coincides with deceasing n_{junct} (Table 1). It is different from the sequence $SP \rightarrow SD \rightarrow DG$ predicted by coarse-grain simulation by the position of the DG.¹⁹ This is attributed to the planarity of the trigonal junctions, being the only one allowing elliptical deformation and thus maintaining a larger number of cohesive glycerols at the junctions than SD. It appears that single networks are generally preferred for the network phases of bolapolyphiles. Though the phase transition sequence is same as in Bonnet transformation, 13b the phase is not controlled by minimal surface transformation. Instead, the phase transition behaves as a result of competition between interfacial tension and space filling.

It is noted, that the network phases discussed here are different from the bicontinuous cubic phases formed by molecular and macromolecular amphiphiles, because the networks are not continuous, but segmented into the polar (slightly deformed) spheres and the rod-bundles with fixed length forming the edges. Two interfaces are generated in these cubic phases; one is between polar glycerols and rigid aromatics and another is between aromatics and alkyl chains. The interfacial tension is a key factor influencing the cubic network phase behaviour based on SCFT.²⁰ Minimizing the interfacial tension requires minimization of interfacial surface area. The aromatic/alkyl interface contributes to the network phase related to the minimal surface. And the glycerol/aromatic interface is defined by network junction shape. Clearly, larger valency induces more spherical junctions, which decreases the interfacial tension and leads to a SP phase as the first network phase and a SD phase upon chain elongation. The DG, usually representing the dominant network phase, is considered as an intermediate structure in this case.

Except for the junction shape, alkyl chain volume also affects the phase behaviour. The experimentally observed sequence SP→DG→SD is in good agreement with predictions based on the development of the radial distribution of the side chain volume dV/dr^{15} , where V(r) is the segment of the unit cell volume within a distance *r* from the closest network segment. Fig. 3 shows the dV/dr curves for the three cubic phases. The SD phase requires longer alkyl chains compared with SP, in line with the molecular design. The intersections between curves and x-axis give an impression on the furthest distance from the network (Table S5, ESI), which reflects the degree of alkyl chain stretching. For SP, the steep increase of dV/dr curve indicates a rapid volume expansion. Meanwhile, alkyl chains are forced to stretch strongly to fill the free volume. The entropy penalty from alkyl chains stretching competes with the enthalpy gain from the glycerols size and shape optimization. The entropic penalty lowers the phase stability, generating lowest Cub-Iso transition point for SP. Upon alkyl chain elongation, DG replaces SP as the alkyl chain entropy penalty can be greatly relieved due to less requirement of chain stretching. Upon further chain elongation, SD becomes a stable phase balancing the junction shape and alkyl chain size.

COMMUNICATION

This article is licensed under a Creative Commons Attribution 3.0 Unported Licence.

Access Article. Published on 21 Ngberere 2025. Downloaded on 29/10/2025 20:52:46.

Journal Name

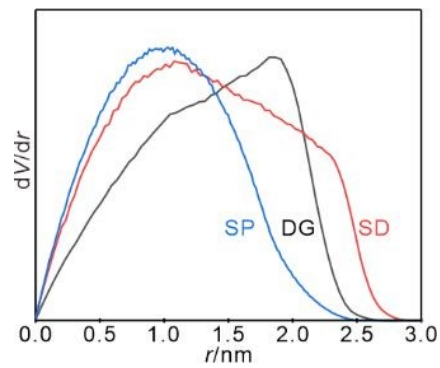


Figure 3. Radial distribution dV/dr for network phases, where V(r) is the unit cell volume within a distance r from the closest network segment. The intersections of the curves on x-axis show the furthest distance from the networks in lattice.

The fixed length of the relatively long BT rods has an additional effect on network formation. While for compounds with relatively short biphenyl and p-terphenyl rods exclusively 3- and 4-way junctions were observed (DG,21 DD,22 SD15), formation of the SP network with 6-way junctions obviously requires the longer BT core,16 while the I-WP23 and A1524 networks with 8- and 12+14-way junctions, respectively, require even longer oligo(phenylene-ethynylene) (OPE) cores involving 5 benzene rings. Similarly, only double networks can be found for biphenyl-based BPs,^{21,22} while p-terphenyl¹⁵ and BT-based cores¹⁶ allow double as well as single network phases, and for the even longer OPE based ${\rm BPs^{23,24}}$ only the high valence single networks I-WP and A15 were found so far. For shorter rods the side chains are closer to the junction points which limits the possible junction valence due to the arising packing frustration.

In summary, a sequence of three different self-assembled LC network phases was obtained (Fig. 2). Two of them represent the rare single networks (SD, SP), in this case accessible by thermodynamically driven self-assembly in a bottom-up approach. The two single network phases are separated by the double gyroid phase as intermediate structure at the transition of the junction valence from 6 to 4. Further chain length variations could provide additional new network structures. Especially elongation beyond n = 30 could possibly lead to the still elusive cubic LC phase with a SG network, which would be of significant interest for energy and environmental science.²⁵

This work is supported by the Deutsche Forschungsgemeinschaft (DFG, 346494874-GRK 2670) and the National Natural Science Foundation of China (No. 12204369). We thank the Shanghai Synchrotron Radiation Facility of BL16B1 (https://cstr.cn/31124.02. SSRF.BL16B1) for assistance on SAXS measurements.

Data Availability Statement

The data supporting this article have been included as part of the Supplementary Information.

Conflicts of interest

There are no conflicts to declare.

View Article Online DOI: 10.1039/D5CC04931H

Notes and references

- M. Newman, Networks, 2nd Ed. Oxford University press, Oxford, 2018.
- (a) T. Ichikawa, T. Kato and H. Ohno, Chem. Commun. 2019, 55, 8205; (b) T. Kato, J. Uchida, T. Ichikawa and T. Sakamoto, Angew. Chem. Int. Ed. 2018, 57, 4355.
- O. Kwon, X. Cai, W. Qu, F. Liu, J. Szydłowska, E. Gorecka, M. J. Han, D. K. Yoon, S. Poppe and C. Tschierske, Adv. Funct. Mater. 2021. 2102271
- C. Tschierske and C. Dressel, Symmetry 2020, 12, 1098.
- M. Maldovan and E. L. Thomas, Nat. Mater. 2004, 3, 593.
- L. Han and S. Che, Adv. Mater. 2018, 30, 1705708.
- Y. Ishii, N. Matubayasi, G. Watanabe, T. Kato and H. Washizu, Sci. Adv. 2021, 7, eabf0669.
 - V. Luzzati, H. Delacroix, A. Gulik, T. Gulik-Krzywicki, P. Mariani and R. Vargas, Stud. Surf. Sci. Catal. 2004, 148, 17.
- J. M. Seddon and R. H. Templer, in Handbook of Biological Physics, ed. R. Lipowsky and E. Sackmann, Elsevier, 1995, vol. 1, pp. 97-
- (a) A. J. Meuler M. A. Hillmyer and F. S. Bates, Macromolecules 2009, 42, 7221; (b) L. Xiang, Q. Li, C. Li, Q. Yang, F. Xu and Y. Mai, Adv. Mater. 2023, 35, 2207684; (c) H. Lee, J. Kim, and M. J. Park, Phys. Rev. Mat. 2024, 8, 020302
- 11 (a) S. Kutsumizu, Isr. J. Chem. 2012, 52, 844; (b) G. Ungar, F. Liu and X. B. Zeng, in Handbook of Liquid Crystals, Vol. 5, 2nd ed. (Eds.: J. W. Goodby, P. J. Collings, T. Kato, C. Tschierske, H. F. Gleeson and P. Raynes), Wiley-VCH, Weinheim 2014.
- 12 H. Lee, S. Kwon, J. Min, S.-M. Jin, J. H. Hwang, E. Lee, W. B. Lee, M. J. Park, Science 2024, 383, 70.
- 13 (a) C. V. Kulkarni, T.-Y. Tang, A. M. Seddon, J. M. Seddon, O. Ces and R. H. Templer, Soft Matter 2010, 6, 3191; (b) C. V. Kulkarni, Langmuir, 2011, 27, 11790.
- 14 C.-Y. Chang, G.-M. Manesi, C.-Y. Yang, Y.C. Hung, K.-C. Yang, P.-T. Chiu, A. Avgeropoulos and R.-M. Ho, PNAS, 2021, 118, e2022275118.
- 15 (a) X. Zeng, S. Poppe, A. Lehmann, M. Prehm, C. Chen, F. Liu, H. Lu, G. Ungar and C. Tschierske, Angew. Chem. Int. Ed. 2019, 58, 7375; (b) S. Poppe, A. Lehmann, M. Steimecke, M. Prehm, Y. Zhao, C. Chen, F. Liu and C. Tschierske, Giant, 2024, 18, 100254; (c) S. Poppe, C. Chen, Y. Cao, F. Liu and C. Tschierske, Small Sci. 2025, 5, 2500157.
- 16 S. Poppe, X. Cheng, C. Chen, X. Zeng, R. Zang, F. Liu, G. Ungar and C. Tschierske, J. Am. Chem. Soc. 2020, 142, 3296.
- 17 (a) C. Tschierske, Chem. Soc. Rev. 2007, 36, 1930-1970 (b) C. Tschierske, C. Nürnberger, H. Ebert, B. Glettner, M. Prehm, F. Liu, X.-B. Zeng and G. Ungar, Interface Focus 2012, 2, 669.
- 18 P. M. Duesing, R. H. Templer and J. M. Seddon, Langmuir 1997, 13, 351.
- Y. Sun, P. Padmanabhan, M. Misra and F. A. Escobedo, Soft Matter 2017, 13, 8542.
- 20 P. Chen, M. K. Mahanthappa and K. D. Dorfman, J. Polym. Sci. **2022**. 60. 2543.
- 21 (a) F. Liu, M. Prehm, X. Zeng, C. Tschierske and G. Ungar, J. Am. Chem. Soc. 2014, 136, 6846; (b) S. Poppe, C. Chen, F. Liu and C. Tschierske, Chem. Commun. 2018, 54, 11196.
- 22 X. Zeng, M. Prehm, G. Ungar, C. Tschierske and F. Liu, Angew. Chem. Int. Ed. 2016, 55, 8324.
- 23 C. Chen, M. Poppe, S. Poppe, C. Tschierske and F. Liu, Angew. Chem. Int. Ed. 2020, 59, 20820.
- (a) C. Chen, M. Poppe, S. Poppe, M. Wagner, C. Tschierske and F. Liu, Angew. Chem. Int. Ed. 2022, 61, e202203447; (b) C. Anders, T. Tan, V.-M. Fischer, R. Wang, M. Alaasar, R. Waldecker, Y. Cao, F. Liu and C. Tschierske, Aggregate 2025, 6, 728.
- 25 C. Bao, S. Che and L. Han, J. Hazar. Mater. 2021, 402, 123538.

• The data supporting this article have been included as part of the Supplementary Information.

View Article Online DOI: 10.1039/D5CC04931H